Pd supported on Zn^{II}–Cr^{III} mixed oxide as a catalyst for one-step synthesis of methyl isobutyl ketone

Fahd Al-Wadaani, Elena F. Kozhevnikova, Ivan V. Kozhevnikov *

Department of Chemistry, University of Liverpool, Liverpool L69 7ZD, UK

ABSTRACT

Pd metal supported on Zn^{II}–Cr^{III} mixed oxide is an efficient bifunctional catalyst for the one-step synthesis of methyl isobutyl ketone (MIBK) from acetone and H$_2$ in the gas and liquid phases. The reaction involves acid-catalysed condensation of acetone to mesityl oxide, followed by its hydrogenation to MIBK. Diisobutyl ketone (DIBK) is a useful byproduct in this process. Zn–Cr oxides (Zn/Cr = 20:1–1:30) are prepared by coprecipitation of Zn^{II} and Cr^{III} hydroxides. The texture and acid properties (i.e., the nature, density, and strength of acid sites) of Zn–Cr oxides, as well as the Pd dispersion in the catalysts, are thoroughly characterised. For both the continuous gas-phase process and the batch liquid-phase process, the preferred catalyst formulation is 0.3 wt% Pd on the amorphous Zn–Cr (1:1) oxide ($S_{BET} = 132$ m^2/g) having Lewis acid sites (1.2 mmol/g density) with an enthalpy of NH$_3$ adsorption of -155 kJ/mol. Both processes produce MIBK with a selectivity of 70–78% and 90% MIBK + DIBK total selectivity at 38–40% acetone conversion. Evidence is provided that hydrogenation of mesityl oxide to MIBK is the rate-limiting step in the gas-phase process.

© 2008 Elsevier Inc. All rights reserved.

1. Introduction

Methyl isobutyl ketone (MIBK) is produced on industrial scale and widely used as a solvent for paint and protective coatings [1]. Traditionally, MIBK is manufactured via a three-step process involving base-catalysed aldol condensation of acetone to diacetone alcohol (DA), acid-catalysed dehydration of DA to mesityl oxide (MO), and metal-catalysed hydrogenation of MO to MIBK [2] (Scheme 1). The use of homogeneous acid and base catalysts causes pollution as well as corrosion problems. Heterogeneous multifunctional catalysts that contain acid–base and metal functionalities and thus are capable of carrying out all three reactions in one step in the liquid or gas phase without separating the intermediate DA and MO have attracted considerable interest [2]. Although the formation of DA and MO is limited by thermodynamically unfavourable equilibria [3], the overall one-step process is exothermic ($\Delta H = -117$ kJ/mol) [2]. It is the downhill hydrogenation of MO to MIBK that drives the one-step process forward. In one-step synthesis of MIBK, diisobutyl ketone (DIBK) also forms as a useful consecutive byproduct, which is a good solvent for various natural and synthetic resins. The one-step process in the liquid phase is operated at 120–200 °C and 20–50 bar H$_2$ pressure, using bifunctional acid–base/redox catalysts composed of acidic cation-exchangers, zeolites, or zirconium phosphate with addition

of platinum group metals, typically palladium [2]. One-step synthesis of MIBK in the gas phase also has attracted interest; however, the MIBK selectivity is generally lower than in the liquid-phase process, and catalyst deactivation may be a problem. Because the one-step process is simpler and more economical, there is an incentive to find new, more efficient catalysts for this process.

In a broader sense, the development of one-step (one-pot) processes with no intermediate separation steps using multifunctional catalysts is important strategy for achieving sustainable organic synthesis with high atom and energy efficiency [4,5]. Multifunctional catalysis can play a key role in the production of value-added chemicals from renewable feedstocks [6]. In this context, the one-step synthesis of MIBK is a good model reaction for probing multifunctional catalysts in both gas and liquid phases.

Numerous bifunctional catalysts have been studied in one-step synthesis of MIBK in both gas- and liquid-phase reactions [7–22]. These include Pt supported on a gallosilicate and alminosilicate [8], NaX and CsX zeolites [9]; Pd on ZSM-5 [10], SAPO-11 [11], AlPO-11 [11], zirconium phosphate [18], niobic acid [19,20] and heteropoly acid [21]; and Pd, Ni, Cu, or Pd-Cu supported on MgO, Mg/Al hydrotalcite, and alumina [7,12–17,22].

Recently, palladium supported on a ZnO–Cr$_2$O$_3$ mixed oxide (Zn/Cr = 1:10 mol/mol) has been reported to be a new, efficient bifunctional catalyst for the one-step synthesis of MIBK in the gas and liquid phases [23]. We report an in-depth investigation of this catalyst system, focusing on catalyst optimisation with respect to the Zn/Cr ratio and Pd loading, complemented by thorough char-
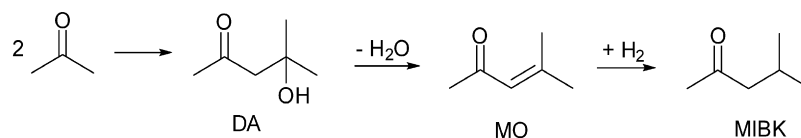
Scheme 1.

Table 1
Catalyst characterisation

Catalyst	S_{BET} (m^2/g)	Pore diameter[a] (Å)	Pore volume[b] (cm^3/g)	H_2O content[c] (wt%)	Density (g/cm^3)	D[d]
Zn–Cr (1:30)	223	29	0.16	8.95		
Zn–Cr (1:10)	193	31	0.15	9.19		
Zn–Cr (1:1)	132	33	0.11	8.97		
Zn–Cr (10:1)	33	112	0.09	2.83		
Zn–Cr (20:1)	36	91	0.08	2.02		
0.3% Pd/Zn–Cr (1:30)	189	36	0.16		1.38	0.83
0.3% Pd/Zn–Cr (1:10)	180	31	0.14		1.39	0.79
0.1% Pd/Zn–Cr (1:1)	99	26	0.06	8.56		0.66
0.3% Pd/Zn–Cr (1:1)	112	35	0.09	9.32	1.44	0.37
1.0% Pd/Zn–Cr (1:1)	107	26	0.07	8.52		0.07
0.3% Pd/Zn–Cr (10:1)	32	103	0.09		1.30	0.58
0.3% Pd/Zn–Cr (20:1)	19	87	0.04		1.73	0.58

[a] Average pore diameter by BET method.
[b] Single point total pore volume.
[c] From TGA as weight loss in the temperature range of 30–600 °C.
[d] Pd dispersion (average values from at least two measurements).

acterisation of catalyst texture, acid properties (type, density and strength of acid sites) and Pd dispersion, along with some mechanistic insights.

2. Experimental

2.1. Catalyst preparation

A series of Zn–Cr mixed oxides with a Zn/Cr atomic ratio of 1:30–20:1 were prepared by coprecipitation of Zn^{II} and Cr^{III} hydroxides as described previously [23]. The coprecipitation was carried out by adding 10 wt% aqueous ammonium hydroxide dropwise to a stirred aqueous solution of a mixture of $Zn^{II} + Cr^{III}$ nitrates $([Zn^{II}] + [Cr^{III}] = 0.2$ M) at 70 °C until pH 7 was achieved, followed by aging the suspension for 3 h at 70 °C. The precipitates were filtered off, washed with deionised water until ammonia-free, dried in air at 100–110 °C overnight, and finally calcined under nitrogen flow for 5 h at 300 °C, yielding Zn–Cr oxides as black powders. The oxides were pelleted and ground into a powder with particle sizes of 45–180 µm. The Pd-doped catalysts were prepared by impregnating Zn–Cr oxides with a 0.02 M solution of $Pd(OAc)_2$ in benzene at room temperature, followed by evaporation of the solvent in a rotary evaporator and subsequent reduction of Pd^{II} to Pd^0 in a hydrogen flow (30 ml/min) at 250 °C for 2 h. The catalysts were stored in a desiccator over P_2O_5. Catalyst characterisation is summarised in Table 1.

2.2. Techniques

The surface area and porosity of Zn–Cr oxides and Pd/Zn–Cr catalysts were measured by nitrogen physisorption at 77 K on a Micromeritics ASAP 2000 instrument. Before the analysis, the samples were evacuated at 250 °C for 3 h. Water content in the catalysts was measured by thermogravimetric analysis (TGA) under nitrogen flow using a Perkin–Elmer TGA 7 instrument. The amount of carbon deposited on the postreactor catalysts was measured by elemental analysis. Powder X-ray diffraction (XRD) spectra of catalysts were recorded on a PANalytical Xpert diffractometer with a

monochromatic $CoK_{\alpha 1}$ radiation $(\lambda = 1.789$ Å). XRD patterns were attributed using the JCPDS database. ICP analysis was carried out on a Spectro Ciros emission spectrometer.

Ammonia adsorption onto the catalysts was measured in a flow system using a Setaram TG-DSC 111 differential scanning calorimeter. The total number of Brønsted and Lewis acid sites in Zn–Cr oxides was measured by passing a continuous flow of NH_3 gas over catalyst samples, as described in detail elsewhere [24]. A pulse method was used for measuring differential heats of NH_3 adsorption (molar heat for each dose of adsorbate). Catalyst samples (60–80 mg) were placed in the calorimeter and pretreated under a flow of helium (30 ml/min) at 300 °C for 1 h. Then the temperature was lowered to 100 °C under a flow of He. After sample weight stabilisation at 100 °C (about 2 h), the analysis was performed by successive pulses of 2 ml of ammonia into the He flow using a loop fitted in a 6-port valve. Sufficient time was allowed after each pulse for adsorption equilibrium to be reached (about 20 min). Weight gain and corresponding heat of adsorption were recorded, from which the differential adsorption heat was obtained.

A Setaram C80 heat flux Calvet type microcalorimeter was used to measure the heat of adsorption of pyridine on Zn–Cr (1:1) and (1:10) oxides in cyclohexane slurry, as described previously [24]. Before these measurements, the samples were pretreated at 200 °C under vacuum. The measurement was carried out at 50 °C. A fresh oxide sample (0.5 g) was used for each adsorption measurement. The amount of adsorbed pyridine was obtained by difference between the amounts of total and unadsorbed pyridine. The latter was measured by UV–vis spectroscopy using a Varian Cary 50 spectrophotometer in a 1-cm quartz cuvette at a pyridine absorption band of 250 nm $(\varepsilon = 1818$ l/(mol cm)).

DRIFT spectra of adsorbed pyridine were obtained using a Nicolet Nexus FTIR spectrometer equipped with a controlled environment chamber (Spectra-Tech model 0030-101). Catalyst samples were diluted with KBr powder (10 wt% in KBr), then loaded into the environmental chamber and pretreated at 100 °C and 20 mTorr for 1 h. Then the background DRIFT spectra were recorded at 100 °C and 20 mTorr. The samples were then exposed to pyridine vapour at 15 Torr pressure and 100 °C for 0.5 h, followed by pumping out at 100 °C and 20 mTorr pressure for 0.5 h. The DRIFT spectra of adsorbed pyridine were recorded at 100 °C and 20 mTorr against the background spectra and displayed in the absorbance mode [i.e., $\log_{10}(1/R)$], where R is the reflectance. Variations in catalyst concentration from 5–50 wt% in KBr did not affect the spectra of adsorbed pyridine apart from the intensity and signal-to-noise ratio, indicating that dilution with KBr did not change the catalysts.

Palladium dispersion in the catalysts was determined by hydrogen chemisorption measured by the pulse technique using a Micromeritics TPD/TPR 2900 instrument, as described elsewhere [25]. Before adsorption of H_2, the catalyst samples were treated in an H_2 flow at 250 °C for 1 h, then exposed to air for 1 h at room temperature to adsorb oxygen on the Pd surface. The dispersion, D, defined as the fraction of palladium at the surface, $D = Pd_s/Pd_{total}$, was calculated assuming the stoichiometry of H_2 adsorption: $Pd_sO + 1.5H_2 \rightarrow Pd_sH + H_2O$ [26].

2.3. Catalyst testing for MIBK synthesis

2.3.1. Gas-phase process

The catalytic tests were performed under atmospheric pressure in a Pyrex glass fixed-bed microreactor (9 mm i.d.) by online gas chromatography (GC) using a Varian Star 3400 CX gas chromatograph equipped with a 30 m × 0.25 mm BP5 capillary column and a flame ionisation detector. The reactor was placed in a vertical tubular furnace. Unless stated otherwise, the catalyst bed contained 0.2 g of a catalyst powder (45–180 μm particle size) placed in the reactor between two layers of Pyrex glass wool. In some cases, the catalyst was diluted by acid-washed sand, which itself was inactive in the reaction. The temperature in the reactor was controlled by a Eurotherm controller using a thermocouple placed at the top of the catalyst bed. The gas feed was fed into the reactor from the top. Acetone was supplied to the gas flow by bubbling a flow of H_2 (10–30 ml/min, controlled by Brooks mass flow controllers) through a stainless steel saturator containing acetone, which was kept at a specific temperature to maintain the chosen acetone vapour pressure. All gas lines were made of stainless steel. The downstream lines and sampling valves were heated at 175 °C to prevent product condensation. Before reaction, the catalysts were pretreated with hydrogen (10–30 ml/min) at 300 °C for 0.5 h. At regular time intervals, the downstream gas flow was analysed by online GC. The liquid products were collected in an ice trap and also analysed by offline GC using a 30 m × 0.25 mm HP-INNOWAX capillary column. The products were identified by GC and GC-MS using authentic samples. The reaction activation energy, E_a, was measured under differential conditions at an acetone conversion ⩽10% using 0.02-g catalyst samples diluted with 0.2 g of sand.

2.3.2. Liquid-phase process

The liquid-phase synthesis of MIBK was carried out in a 45-ml Parr 4714 stainless steel autoclave equipped with a pressure gauge and a magnetic stirrer. Tests using the glass-lined autoclave revealed no effect of the stainless steel on the reaction with Pd/Zn–Cr catalysts. However, the reaction with Zn–Cr oxides in the absence of Pd was carried out in the glass-lined reactor to avoid any effect of Pd contamination. Typically, the reaction mixture contained 2.0 g of acetone, 0.30 g of decane (internal GC standard), and 0.20 g of catalyst. The stirring speed was 800 rpm unless stated otherwise. The autoclave was purged three times with H_2, then pressurised with H_2 and placed in an oil bath, preheated to the reaction temperature. Judging from the resulting pressure, most of the acetone remained liquid under such conditions. After completion of the reaction, the reactor was cooled with ice to 0 °C, depressurised in a gas bag with a stopcock to collect gaseous products (propene and propane), and opened. The reaction mixture was then removed from the autoclave and separated from the catalyst by centrifugation. Products were identified by GC-MS and quantified by GC, using a Varian Star 3400 CX instrument equipped with a flame ionisation detector and a 30 m × 0.25 mm HP-INNOWAX capillary column.

3. Results and discussion

3.1. Catalyst characterisation

Zn–Cr oxides with a Zn/Cr atomic ratio of 1:30–20:1 were prepared by coprecipitation of Zn^{II} and Cr^{III} hydroxides, followed by calcination at 300 °C. Zn-rich oxides (Zn/Cr = 10:1–20:1) were crystalline materials, exhibiting the XRD pattern of ZnO crystalline phase (Fig. 1). In contrast, Cr-rich oxides (Zn/Cr = 1:1–1:30) were amorphous materials (Fig. 1). Calcination of Zn–Cr oxides at higher temperatures (>350 °C) yields crystalline materials
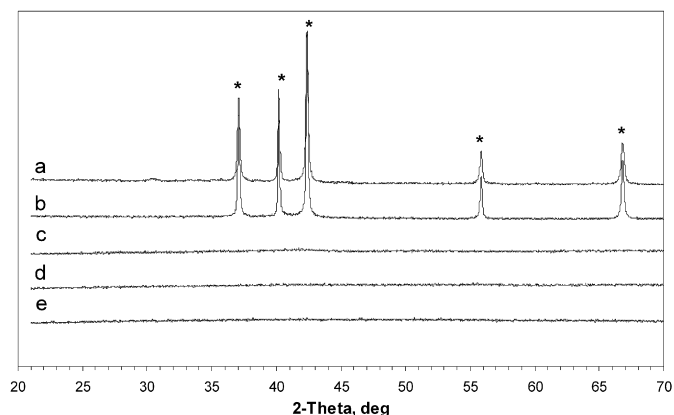

Fig. 1. XRD for Zn–Cr oxides: (a) Zn–Cr (20:1), (b) Zn–Cr (10:1), (c) Zn–Cr (1:1), Zn–Cr (1:10), Zn–Cr (1:30). ZnO pattern is asterisked.

comprising ZnO, $ZnCr_2O_4$ and Cr_2O_3 phases ([23] and references therein). The crystalline Zn–Cr (1:10) oxide has been found to have a smaller surface area and a lower catalytic activity in MIBK synthesis compared with the amorphous Zn–Cr (1:10) oxide [23].

The texture of Zn–Cr oxides was characterised by N_2 physisorption. The amorphous Cr-rich oxides had greater surface areas (132–223 m^2/g) and pore volumes (0.11–0.16 cm^3/g) but smaller average pore diameters (29–33 Å) than the crystalline Zn-rich oxides (33–36 m^2/g, 0.08–0.09 cm^3/g, and 91–112 Å, respectively) (Table 1). The surface area of the Cr-rich oxides increased significantly with increasing the Cr content. The pore structure of the Zn–Cr oxides was found to depend on their Zn/Cr ratio, as evidenced by the pore volume distributions (Fig. 2). The Cr-rich amorphous oxides had a more regular pore structure in which pores of 35–37 Å diameter dominated, with smaller pores also present. Pores >40 Å in diameter were not found in these oxides. In contrast, the Zn-rich crystalline oxides had a much broader pore size distribution (Fig. 2). These oxides exhibited a sharp peak at a 37–38 Å pore diameter, like the Cr-rich oxides, but also had larger pores of up to 1000 Å diameter (Fig. 2), hence the larger average pore diameter. The Zn–Cr (10:1) oxide exhibited a broad peak centred at 91 Å pore diameter. Palladium loading did not change the catalyst texture but slightly decreased the surface area and pore volume, as expected (Table 1). The Cr-rich catalysts had a density of 1.38–1.44 g/cm^3, whereas the Zn-rich catalysts were lighter, with a density of 0.77–1.30 g/cm^3 (Table 1).

TGA analysis of Zn–Cr oxides and Pd/Zn–Cr catalysts showed a monotonous loss of water in the temperature range of 30–600 °C (Fig. 3). The amount of water depended on the Zn/Cr ratio: ~9 wt% for the amorphous oxides (Zn/Cr = 1:30–1:1) and 2.0–2.8 wt% for crystalline (Zn/Cr = 10:1–20:1) (Table 1).

Table 2 summarizes the acid properties of Zn–Cr oxides. The total number of acid sites, as determined from NH_3 adsorption in a gas/solid flow system at 100 °C, decreased with decreasing the Cr content from 2.4 mmol/g (Zn/Cr = 1:30) to 0.3 mmol/g (Zn/Cr = 20:1) in parallel with the oxide surface area. The nature of acid sites (Brønsted or Lewis) was determined by FTIR spectroscopy of adsorbed pyridine [27]. The entire series of Zn–Cr oxides was found to have Lewis acid sites, as evidenced by the presence of the adsorption band at 1450 cm^{-1} in their spectra (Fig. 4). Only one oxide, Zn–Cr (1:30), with the largest Cr content, had Brønsted acid sites of sufficient strength to protonate pyridine, as indicated by the band at 1540 cm^{-1} in the spectrum of this oxide (Fig. 4e).

The strength of acid sites was characterised by ammonia adsorption calorimetry. Although they cannot differentiate between Brønsted and Lewis acid sites, these measurements provide a profile of adsorption enthalpy (i.e., acid strength) as a function of NH_3
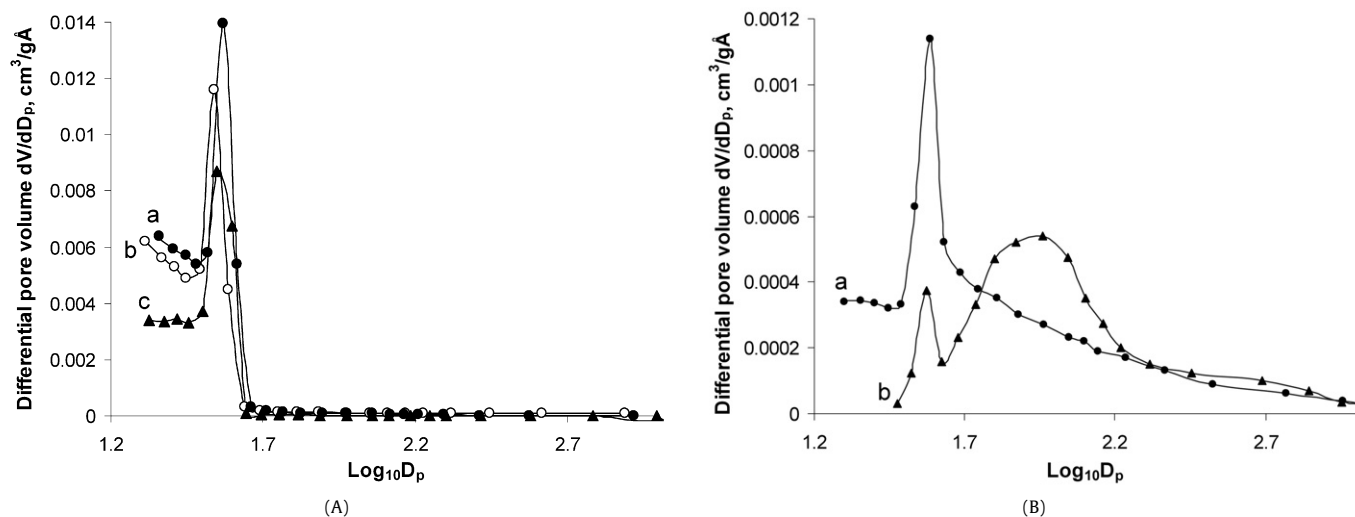
Fig. 2. Distribution of pore volume as a function of pore diameter, D_p (in Å), for Zn–Cr oxides obtained by BJH method from nitrogen desorption. (A): (a) Zn–Cr (1:10), (b) Zn–Cr (1:30), (c) Zn–Cr (1:1). (B): (a) Zn–Cr (20:1), (b) Zn–Cr (10:1).
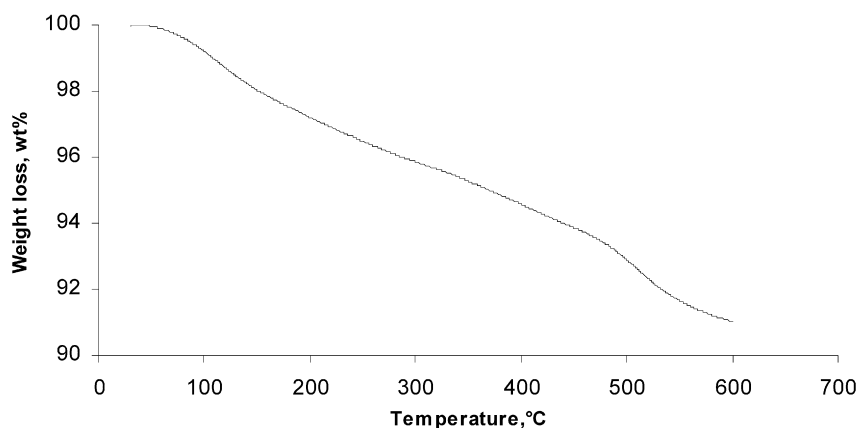

Fig. 3. TGA for Zn–Cr (1:1) oxide.

Table 2
Acid properties of Zn–Cr oxide

Zn–Cr oxide	Acid site density[a] (mmol/g)	Acid site type[b]	ΔH (NH$_3$)[c] (kJ/mol)	ΔH (Py)[d] (kJ/mol)
Zn–Cr (1:30)	2.4	B + L	−193	
Zn–Cr (1:10)	1.8	L	−180	−129
Zn–Cr (1:1)	1.2	L	−155	−106
Zn–Cr (10:1)	1.0	L	−150	
Zn–Cr (20:1)	0.3	L	−127	

[a] From NH$_3$ adsorption at 100 °C.
[b] Brønsted (B) and Lewis (L) acid sites from FTIR of adsorbed pyridine.
[c] Initial enthalpy of NH$_3$ adsorption at zero adsorption coverage at 100 °C.
[d] Initial enthalpy of pyridine adsorption at zero adsorption coverage in cyclohexane slurry at 50 °C.

coverage. As an example, Fig. 5 shows the differential adsorption heat as a function of the amount of NH$_3$ adsorbed for Zn–Cr (1:1). The initial enthalpies of NH$_3$ adsorption at zero adsorption coverage were obtained for all Zn–Cr oxides and ranged from −127 to −193 kJ/mol (Table 2). The acid strength, as well as the total number of acid sites, increased with increasing Cr content. Zn–Cr (1:30) oxide had the greatest number of acid sites and the strongest acid sites (both Brønsted and Lewis). All of the other oxides had only Lewis acid sites of a weaker strength.

For Zn–Cr (1:1) and (1:10) oxides, which demonstrated better catalytic performances (see below), the acid strength was also
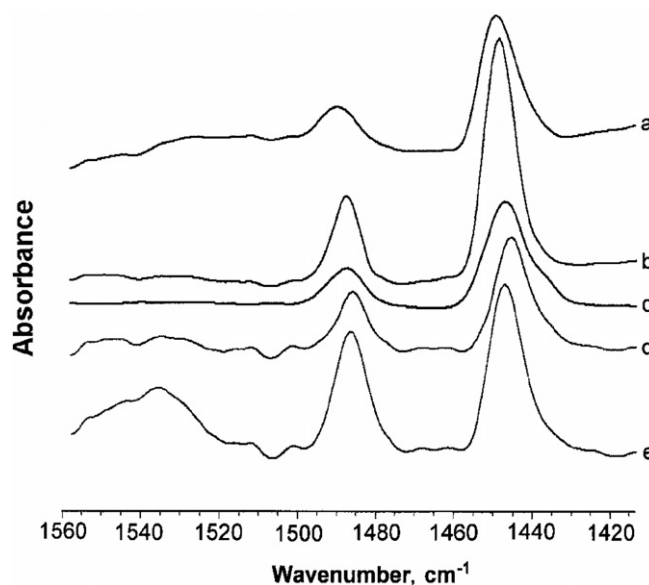

Fig. 4. FTIR spectra of pyridine adsorbed on Zn–Cr oxides with Zn/Cr atomic ratio: (a) 20:1, (b) 10:1, (c) 1:1, (d) 1:10 and (e) 1:30.

determined in liquid phase using microcalorimetry of pyridine adsorption in cyclohexane slurry. These measurements gave an ini-
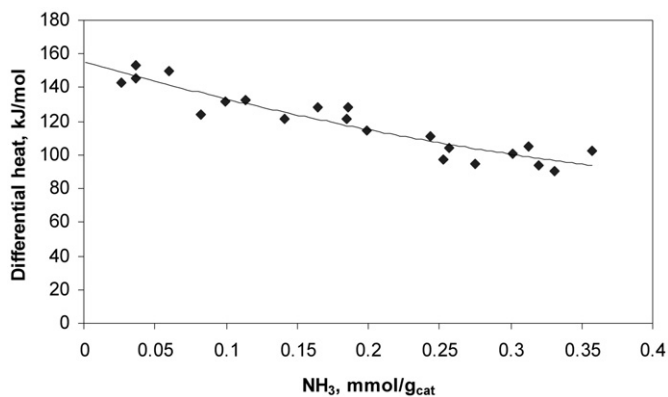
Fig. 5. Differential heat of NH_3 adsorption on Zn–Cr (1:1) at 100 °C.
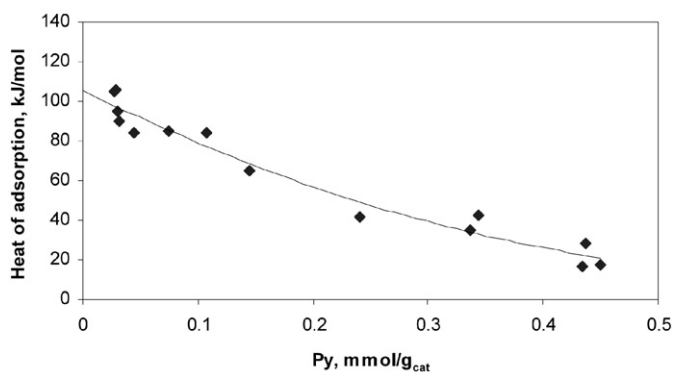

Fig. 6. Heat of pyridine adsorption on Zn–Cr (1:1) in cyclohexane slurry at 50 °C.

tial adsorption enthalpy of −106 kJ/mol for Zn–Cr (1:1) oxide and −129 kJ/mol for Zn–Cr (1:10) oxide (Table 2). Fig. 6 shows the adsorption heat as a function of the amount of pyridine adsorbed for Zn–Cr (1:1).

Palladium dispersion, D, in Pd/Zn–Cr catalysts (0.1–1 wt% Pd) was obtained by measuring hydrogen chemisorption. The D values are given in Table 1. At a constant Pd loading of 0.3 wt%, the dispersion decreased with decreasing the Cr content in Zn–Cr oxides. This can be explained by the decrease in oxide surface area in this direction. As expected, Pd dispersion decreased with increasing Pd loading from 0.1 to 1.0 wt% on Zn–Cr (1:1) oxide.

3.2. Gas-phase synthesis of MIBK

The gas-phase reaction was studied in a fixed-bed flow reactor under stationary conditions in the temperature range of 200–

350 °C at ambient pressure and an acetone/H_2 molar ratio in the gas feed of 37:63. The GHSV varied from 4000 to 12000 h^{-1}. The Pd loading on Zn–Cr oxides was typically kept at 0.3 wt%. In the case of Zn–Cr (1:1), it was varied from 0.1 to 1 wt% to evaluate the effect of Pd dispersion on catalyst performance.

Representative results at 300 °C are given in Table 3. Both acid and hydrogenation catalysis, effected by Zn–Cr oxide and Pd, respectively, were required for the reaction to occur. When Zn–Cr (1:10) oxide was used in the absence of Pd, the reaction occurred with a low conversion of 16.7% and mesityl oxide (the product of acid-catalysed condensation of acetone) as the major product (63.2% selectivity), with a selectivity to MIBK of only 15.3% (entry 1). This shows that the Zn–Cr oxide itself acted mainly as an acid catalyst, having only weak hydrogenation activity. In the presence of Pd, acetone conversion increased up to 40.5% (entry 3), indicating that the thermodynamically favourable hydrogenation of MO to MIBK on Pd sites was driving the process forward.

The Pd/Zn–Cr catalysts exhibited good performance stability regardless of Zn/Cr ratio. Catalyst deactivation was not observed during at least 10 h of continuous operation (Fig. 7). The catalysts reached steady state in 1–2 h and after that performed with a constant activity and selectivity. Coke (0.7–4.9 wt%) was found in the catalysts after reaction (Table 3), increasing in amount with increasing catalyst acidity, with Pd/Zn–Cr (1:30) and Pd/Zn–Cr (1:10) catalysts depositing larger amounts of coke.

With all of the Pd/Zn–Cr catalysts, MIBK was the major reaction product, with significant amounts of DIBK also formed. Byproducts included C_{9+} acetone condensation products (mainly 2,6,8-trimethylnonane-4-one and some mesitylene) together with small amounts of propene and propane (C_3), mesityl oxide (MO), and isopropanol (IP), in agreement with a previous report [23]. The IP formed by direct hydrogenation of the C=O group in acetone on Pd. The C_3 formed by acid-catalysed dehydration of IP to propene on Zn–Cr oxide, followed by hydrogenation of propene to propane on Pd. This was confirmed by the 70–80% conversion of IP to C_3 with >50% selectivity on 0.3% Pd/Zn–Cr (1:1) under the typical reaction conditions (300 °C, 0.2 g catalyst, 1 vol% IP in H_2 flow [10 ml/min], 3 h on stream).

Variation of the Zn/Cr ratio (i.e., catalyst acidity) had a very slight effect on acetone conversion but a considerable effect on reaction selectivity (Table 3, entries 2–4, 9, 10). The catalyst 0.3% Pd/Zn–Cr (1:1) having an intermediate acid strength and acid site density (Table 2) exhibited the highest MIBK selectivity of 70.2%, along with a 90.1% total selectivity to MIBK+DIBK at 39.6% acetone conversion (entry 4). This result compares well with the results reported previously [10,16,19,22].

The Pd dispersion, D, had a profound effect on catalyst activity (Table 3, entries 5–7). The conversion of acetone over Pd/Zn–Cr (1:1) was scaled directly with the amount of accessible surface

Table 3
Gas-phase synthesis of MIBK over Pd/Zn–Cr catalysts[a]

Entry	Catalyst	H_2 flow (ml/min)	Conversion (%)	Selectivity[b] (%)						C[c] (wt%)
				MIBK	DIBK	C_3	IP	MO	Others	
1	Zn–Cr (1:10)	10	16.7	15.3	9.4	0.2	0	63.2	12.0	
2	0.3% Pd/Zn–Cr (1:30)	10	38.7	64.8	18.5	0.7	3.3	3.1	9.6	4.1
3	0.3% Pd/Zn–Cr (1:10)	10	40.5	58.7	20.7	0.6	4.1	3.0	12.9	4.9
4	0.3% Pd/Zn–Cr (1:1)	10	39.6	70.2	19.9	0.7	2.5	0.2	6.6	2.6
5	0.3% Pd/Zn–Cr (1:1)	20	34.2	70.7	17.0	1.0	4.1	0.2	6.9	
6	0.1% Pd/Zn–Cr (1:1)	20	20.4	74.4	11.7	3.2	3.8	0.4	6.4	
7	1.0% Pd/Zn–Cr (1:1)	20	18.9	71.3	13.7	2.4	4.5	0.6	7.6	
8	0.3% Pd/Zn–Cr (1:1)	30	30.3	72.2	15.2	1.2	4.3	0.4	6.7	
9	0.3% Pd/Zn–Cr (10:1)	10	35.7	68.7	18.4	0.7	5.0	0.2	6.9	0.7
10	0.3% Pd/Zn–Cr (20:1)	10	40.7	53.3	26.4	1.0	3.9	0	15.4	

[a] Reaction conditions: 300 °C, acetone/H_2 = 37:63 (mol/mol), 0.2 g catalyst of 45–180 µm particle size, 3 h time on stream.
[b] C_3 is propene and propane, IP is isopropanol, MO is mesityl oxide, others are mainly C_{9+} acetone condensation products (mostly 2,6,8-trimethylnonane-4-one).
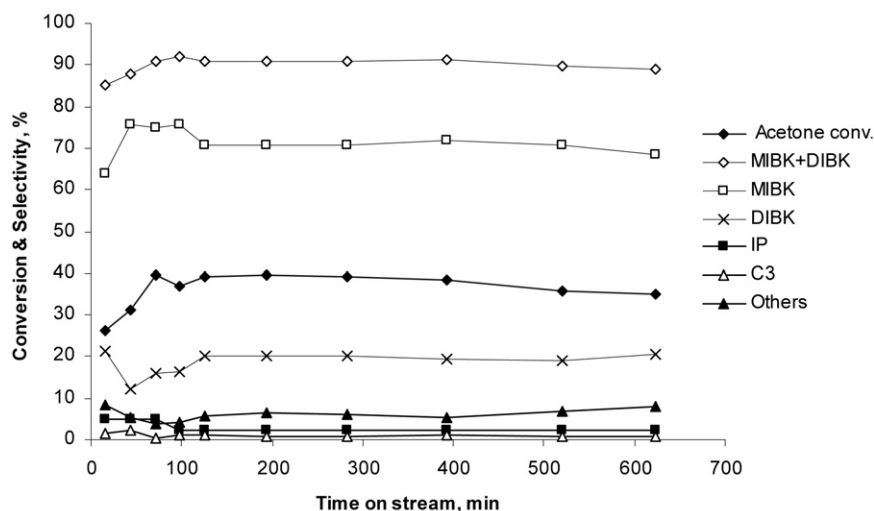[c] Carbon content in used catalysts after 6–8 h on stream.

Fig. 7. Acetone conversion and product selectivities vs time on stream (0.2 g 0.3% Pd/Zn–Cr (1:1), 10 ml/min H_2 flow, acetone/H_2 = 37:63 mol/mol, 300 °C).

Table 4
Effect of flow rate on MIBK synthesis at constant contact time[a]

H_2 flow (ml/min)	Acetone conversion (%)	Selectivity[b] (%)					
		MIBK	DIBK	C_3	IP	MO	Others
10	32.4	69.2	18.3	1.1	3.2	0.2	8.1
20	34.1	68.5	18.6	0.9	3.4	0.2	8.4
30	34.7	67.1	19.2	1.0	3.6	0.2	9.0

[a] Reaction conditions: 0.3% Pd/Zn–Cr (1:1) catalyst (0.1–0.3 g) diluted 50:50 (wt) with sand; the catalyst bed was scaled with H_2 flow rate to keep a constant contact time of 0.3 s; 300 °C, acetone/H_2 = 37:63 (mol/mol), 3.5 h time on stream.
[b] See footnote b in Table 2.

palladium, Pd_s, in the catalysts. Thus, the 0.3% Pd/Zn–Cr (1:1) catalyst ($D = 0.37$), with 0.11 wt% Pd_s exhibited an acetone conversion of 34.2%. This value is proportionally higher than that (20.4%) for the catalyst with 0.1% Pd loading ($D = 0.66$, 0.066 wt% Pd_s) and also that (18.9%) for the catalyst with 1% Pd loading ($D = 0.07$, 0.007 wt% Pd_s). The catalysts with 0.1% and 1% Pd loadings, with equal amounts of Pd_s, exhibited almost equal catalytic activities. This result, together with the independence of catalyst activity on the catalyst acidity, indicates that hydrogenation of MO to MIBK is the rate-limiting step in the process (Scheme 1). This also justifies the Pd loading of 0.3 wt% in the catalysts.

Acetone conversion and product selectivity did not depend on the flow rate at a constant contact time (Table 4), indicating that the reaction was not affected by external mass transfer. The conversion of acetone increased with increasing contact time, with a simultaneous decrease in MIBK selectivity in favour of DIBK (Table 3, entries 4, 5, 8), as would be expected for a consecutive reaction. It should be noted that these tests were carried out under nondifferential conditions, which smoothed the effect of contact time.

The temperature dependence of the reaction rate was studied under differential conditions (acetone conversion ⩽10%) in the temperature range of 200–350 °C using 0.3% Pd/Zn–Cr (1:1) as the catalyst. Under such conditions, the selectivity to MIBK was 79–89%. In the entire temperature range, the reaction obeyed the Arrhenius equation, with an activation energy of 17.0 kJ/mol (Fig. 8). The relatively low value of E_a, together with the previously observed reaction slowdown with increasing catalyst particle size [23], suggests that the reaction may be affected by internal mass transfer.
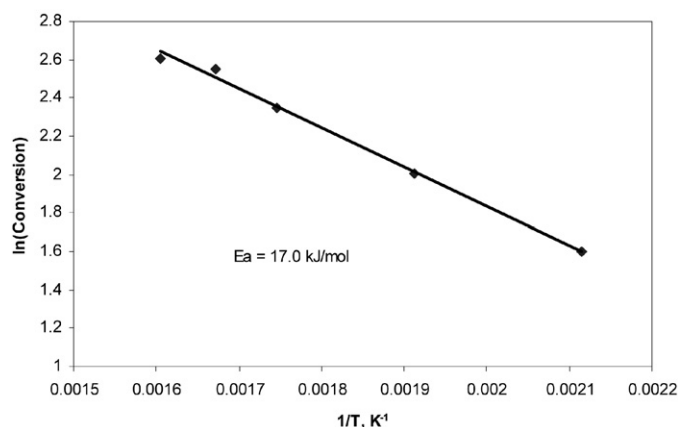

Fig. 8. Arrhenius plot for MIBK synthesis over 0.3% Pd/Zn–Cr (1:1).

3.3. Liquid-phase synthesis of MIBK

The reaction in the liquid phase was carried out in a 45-ml batch reactor (Parr 4714 autoclave) at 180 °C and an initial hydrogen pressure of 7.5 bar at room temperature, with the pressure rising to 14 bar at 180 °C. The stirring speed was 800 rpm, and the gas/liquid volume ratio was 15. Under these conditions, acetone conversion and reaction selectivity did not depend on the stirring speed, indicating absence of mass transfer limitations. The results are summarized in Table 5. Typically, the same reaction products were observed in the liquid phase as in the gas phase, except for more isopropanol and less C_{9+} formed in the liquid phase. In these experiments, the conversion of H_2 was 70–85%, as estimated from the pressure drop occurring during reaction.

As in the gas phase, when Zn–Cr oxide was used without Pd, the reaction occurred with low conversion (17.3%), with mesityl oxide as the major product (72.9% selectivity) and an MIBK selectivity of only 4.9% (entry 1). In the presence of Pd, acetone conversion increased, and MIBK became the main reaction product. In the liquid phase, unlike in the gas phase, increasing the Zn/Cr ratio from 1:30 to 20:1 (i.e., decreasing catalyst acidity) led to a decrease in acetone conversion from 55.8% to 25.8%. As in the gas phase, the 0.3% Pd/Zn–Cr (1:1) catalyst, of intermediate acidity, exhibited the best performance (78.4% MIBK and 90.3% MIBK + DIBK selectivity at 38.3% conversion; entry 5). The more-acidic catalysts 0.3% Pd/Zn–Cr (1:30) and (1:10) were more active but less selective to MIBK and DIBK (entries 2 and 3). The less-acidic 0.3% Pd/Zn–Cr

Table 5
Liquid-phase synthesis of MIBK over Pd/Zn–Cr catalysts[a]

Entry	Catalyst	Conversion (%)	Selectivity (%)[b]					
			MIBK	DIBK	C$_3$	IP	MO	Others
1	Zn:Cr (1:1)	17.3	4.9	0	1.9	11.1	72.9	9.3
2	0.3% Pd/Zn:Cr (1:30)	55.8	66.5	10.5	1.8	4.5	0.6	16.1
3	0.3% Pd/Zn:Cr (1:10)	41.9	72.5	10.9	1.9	7.1	1.2	6.4
4	0.1% Pd/Zn:Cr (1:1)	34.9	75.4	13.1	1.0	3.1	1.3	6.1
5	0.3% Pd/Zn:Cr (1:1)	38.3	78.4	11.9	1.9	4.7	0.8	2.3
6	0.3% Pd/Zn:Cr (1:1)[c]	38.3	59.6	4.4	3.1	30.9	1.7	1.3
7	0.3% Pd/Zn:Cr (1:1)[d]	39.4	60.5	3.4	3.2	31.4	1.3	0.2
8	1% Pd/Zn:Cr (1:1)	36.3	57.4	8.1	1.1	26.8	3.1	3.5
9	0.3% Pd/Zn:Cr (10:1)	34.5	56.3	2.7	2.7	34.3	2.7	1.3
10	0.3% Pd/Zn:Cr (20:1)	25.8	38.9	0.9	1.2	54.6	3.1	1.3

[a] Reactions in 45-ml autoclave, 180 °C, 7.5 bar initial H$_2$ pressure (RT), 2.0 g acetone, 0.20 g catalyst powder of 45–180 μm particle size, 800 rpm stirring speed, 2 h.
[b] C$_3$ is propene and propane, IP isopropanol, MO mesityl oxide, others are mainly C$_{9+}$ acetone condensation products (mostly 2,6,8-trimethylnonane-4-one).
[c] Reuse of entry 4 run; prior to reuse, the catalyst was separated and heated at 150 °C under vacuum for 1 h.
[d] Reuse of entry 4 run; prior to reuse, the catalyst was first treated as in (c) then heated in H$_2$ flow at 250 °C for 1 h.

(10:1) and (20:1) were less active and much less selective, yielding large amounts of IP (entries 9 and 10). Increasing the Pd loading from 0.1% to 1% had little effect on acetone conversion (entries 4, 5, and 8); however, the 1% Pd catalyst was much less selective, giving a large amount of IP (26.8%; entry 8).

We attempted to reuse the 0.3% Pd/Zn–Cr (1:1) catalyst using different pretreatments (Table 5). In one attempt, the catalyst isolated after first run (entry 5) was heated to 150 °C in vacuum for 1 h before reuse (entry 6). Another attempt involved the same heat treatment, followed by heating under a hydrogen flow at 250 °C for 1 h (entry 7). Both attempts gave similar results: Acetone conversion regained its initial level, albeit with reduced MIBK selectivity and an increased amount of IP. This indicates that the postreaction catalyst partly lost its acidity while maintaining high hydrogenation activity.

4. Conclusion

This study has shown that palladium metal supported on Zn–Cr mixed oxide is an efficient bifunctional catalyst for the one-step synthesis of MIBK from acetone and H$_2$ in the gas and liquid phases. Optimisation of catalyst composition has led to the preferred catalyst formulation comprising 0.3% Pd on the amorphous Zn–Cr (1:1) oxide for both gas- and liquid-phase processes. Both the continuous gas-phase process and the batch liquid-phase process produced MIBK with a selectivity of 70–78% and 90% total MIBK + DIBK selectivity at 38–40% acetone conversion, on a par with the best results reported to date.

Acknowledgment

References

[1] W.F. Hoelderich, Stud. Surf. Sci. Catal. 41 (1988) 83.
[2] K. Weissermel, H.-J. Arpe, Industrial Organic Chemistry, fourth ed., Wiley–VCH, Weinheim, 2003.
[3] F. Figueras, J. Lopez, in: R.A. Sheldon, H. van Bekkum (Eds.), Fine Chemicals through Heterogeneous Catalysis, Wiley–VCH, Weinheim, 2001, p. 327.
[4] J.-C. Wasilke, S.J. Obrey, R.T. Baker, G.C. Bazan, Chem. Rev. 105 (2005) 1001.
[5] A. Bruggink, R. Schoevart, T. Kieboom, Org. Process Res. Dev. 7 (2003) 622.
[6] A. Corma, S. Iborra, A. Velty, Chem. Rev. 107 (2007) 2411.
[7] M. Martínez-Ortiz, D. Tichit, P. Gonzalez, B. Cog, J. Mol. Catal. A 201 (2003) 199.
[8] Y. Diaz, L. Melo, M. Mediavilla, A. Albornoz, J.L. Brito, J. Mol. Catal. A 227 (2005) 7.
[9] L.V. Mattos, F.B. Noronha, J.L.F. Monteiro, J. Catal. 209 (2002) 166.
[10] P.Y. Chen, S.J. Chu, C.C. Chen, N.S. Chang, W.C. Lin, T.K. Chuang, US Patent 5059724 (1991).
[11] S.-M. Yang, Y.M. Wu, Appl. Catal. A 192 (2000) 211.
[12] N.N. Das, S.C. Srivastava, Bull. Mater. Sci. 25 (2002) 283.
[13] Y.Z. Chen, C.M. Hwang, C.W. Liaw, Appl. Catal. A 169 (1998) 207.
[14] N. Das, D. Tichit, R. Durand, P. Graffin, B. Coq, Catal. Lett. 71 (2001) 181.
[15] L.M. Gandia, M. Montes, Appl. Catal. A 101 (1993) L1.
[16] V. Chikán, Á. Molnár, K. Baláznik, J. Catal. 184 (1999) 134.
[17] K.H. Lin, A.N. Ko, Appl. Catal. A 147 (1996) L259.
[18] Y. Watanabe, Y. Matsumura, Y. Izumi, Y. Mizutani, J. Catal. 40 (1975) 76.
[19] Y. Higashio, T. Nakayama, Catal. Today 28 (1996) 127.
[20] Y.Z. Chen, B.J. Liaw, H.R. Tan, K.L. Shen, Appl. Catal. A 205 (2001) 61.
[21] R.D. Hetterley, E.F. Kozhevnikova, I.V. Kozhevnikov, Chem. Commun. (2006) 782.
[22] S. Narayanan, R. Unnikrishnan, Appl. Catal. A 145 (1996) 231.
[23] E.F. Kozhevnikova, I.V. Kozhevnikov, J. Catal. 238 (2006) 286.
[24] E.F. Kozhevnikova, I.V. Kozhevnikov, J. Catal. 224 (2004) 164.
[25] M. Musawir, E.F. Kozhevnikova, I.V. Kozhevnikov, J. Mol. Catal. A 262 (2007) 93.
[26] J.E. Benson, H.S. Hwang, M. Boudart, J. Catal. 30 (1973) 146.
[27] K. Tanabe, in: J.R. Anderson, M. Boudart (Eds.), Catalysis Science and Technology, Springer, 1981, chap. 5.